LAWRENCE
LIVERMORE
NATIONAL
LABORATORY

LLNL-PROC-667841

A HIERARCHICAL COMPUTATIONAL THERMODYNAMIC AND KINETIC APPROACH TO DISCONTINUOUS PRECIPITATION IN THE U-NB SYSTEM

T. C. Duong, R. E. Hackenberg, H. M. Volz, A. Llobet, A. I. Smith, G. King, A. Landa, S. Gibbons, S. Bajaj, A. Ruban, L. Vitos, P. E. A. Turchi, R. Arroyave

February 27, 2015

SOLID-SOLID PHASE TRANSFORMATIONS IN INORGANIC MATERIALS, PTM
WHISTLER, Canada
June 28, 2015 through July 3, 2015

Disclaimer

A Hierarchical Computational Thermodynamic and Kinetic Approach to Discontinuous Precipitation in the U-Nb System

T.C. Duong[1], R.E. Hackenberg[2], H.M. Volz [2], A. Llobet[2], A.I. Smith[2], G. King[2], A. Landa[3], S. Gibbons[1], S. Bajaj[4], A. Ruban[5], L. Vitos[5], P.E.A. Turchi[3], R. Arroyave[1]

[1]Texas A&M University (TAMU), College Station, TX, 77840, USA
[2]Los Alamos National Laboratory (LANL), Los Alamos, NM 87545
[3]Lawrence Livermore National Laboratory (LLNL), Livermore, CA 94550
[4]California Institute of Technology (CALTECH), Pasadena, CA 91125
[5]Royal Institute of Technology (KTH), Stockholm, Sweden

Keywords: Discontinuous precipitation, DFT, CALPHAD, PFM

Abstract

U-Nb alloys decompose via discontinuous precipitation (DP) over a broad range of aging conditions, adversely affecting their properties. The growth kinetics, lamellar spacing, and Nb partitioning have been measured, but the thermodynamic and kinetic factors underlying these specific transformation characteristics and reaction paths, vis-a-vis the monotectoid reaction, are not fully resolved. In this work, a hierarchical computational thermodynamic and kinetic approach was carried out to investigate DP. The hierarchical approach started with density-functional theory (DFT) investigations of ground-state formation energies of bcc-based U-Nb alloys. The estimated energetic data was then utilized as an imposed first-principles-based constraint to improve the consistency of the CALPHAD thermodynamic and, subsequently, kinetic assessments of U-Nb. Phase-field simulations were then carried out to study DP's microstructure evolution using the assessed CALPHAD thermodynamic and kinetic representations. Good agreement with experiments on different physical/length scales was achieved, which validates the present theoretical contributions to a better understanding of DP in U-Nb alloys.

Introduction

Among the actinides and age-hardening alloys more broadly, U-Nb is a scientifically interesting material. Depending on the thermal history, the material can undergo different intriguing metastable phase transformations whose resulting microstructures exhibit a rich class of morphologies that strongly affect the material's physical and/or mechanical behaviors. Within this work, we are particularly interested in the U-Nb's DP [1].

DP is the decomposition of a supersaturated solid solution into a solute-depleted matrix and a precipitate phase across a moving boundary [2]. In its simplest form, the precipitation happens as follows:

$$\gamma \rightarrow \alpha + \gamma' \tag{1}$$

where γ is a supersaturated matrix decomposing into stable α precipitate and solute depleted γ'. In U-Nb, DP appears as the result of the discontinuous monotectoid decompo-

sition from a bcc-based Nb-supersaturated U-Nb matrix (γ) into a stable orthorhombic-based Nb-depleted U-Nb precipitate (α) and a bcc-based Nb-enriched U-Nb alloy(γ'), as demonstrated in the schematic phase diagram shown in Fig. 1.

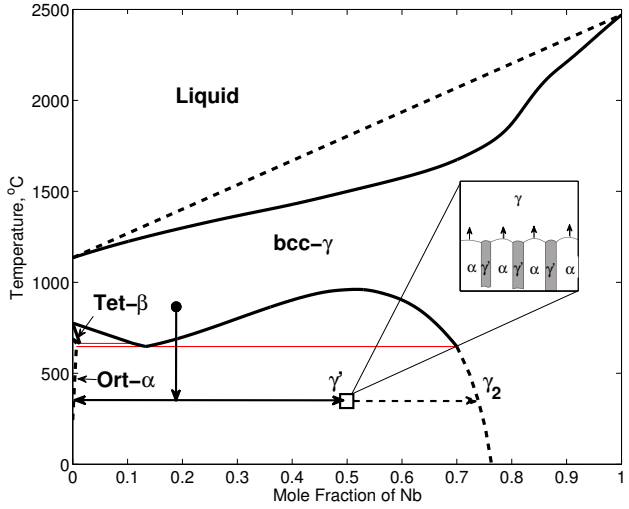

Figure 1: Schematic demonstration of DP in U-Nb.

Questions such as: (1) "how can the metastable γ' exist?" and (2) "what could possibly be the growth mechanism of U-Nb's DP?" require answers, hence a need for understanding the fundamental thermodynamics and kinetics of U-Nb, which tend to be more accessible via theoretical approaches than experiments for this particular system. In the present work, we propose to use a hierarchical computational thermodynamic and kinetic approach to achieve such understanding. This hierarchical approach includes first-principles calculations [3], CALPHAD [4], and phase-field modeling (PFM) [5]. In particular, first-principles calculations were coupled with CALPHAD to assess consistent thermodynamic and kinetic representations of the U-Nb system; In turn, phase-field simulations were carried out by making use of this information to investigate the growth mechanism of metastable γ'. Details on the hierarchical computation and its results are discussed in the next section.

Computational Details

First-Principles Calculations

Isostructural formation energies of γ were evaluated according to the following expression: $\Delta H^{\gamma} = {}^{0}E^{\gamma}_{U_{1-x}Nb_x} - (1-x){}^{0}E^{\gamma}_{U} - x{}^{0}E^{\gamma}_{Nb}$; Where, the ground-state energies ${}^{0}E^{\gamma}$ were calculated using two different Green's function density-functional approaches, namely Korringa-Kohn-Rostoker (KKR) multiple scattering formalism and exact muffin-tin orbital (EMTO) method. The substitutional disorder of the alloys has been treated by using the coherent potential approximation (CPA). The self-consistent calculations were performed within the scalar-relativistic regime for a basis set of *spdf* valence orbitals.

The core states were recalculated at every ionic step according to the soft-core approximation. The generalized gradient approximation (GGA) has been adopted for the exchange-correlation functional. The integration over the Brillouin zone was done using a $31 \times 31 \times 31$ grid of k-points determined according to the Monkhorst-Pack scheme. Integration of the Green's function was carried out over a complex energy contour with a 2.6 Ry diameter using a Gaussian integration technique with 40 points on a semi-circle enclosing the occupied states. Screened Coulomb interactions were taken into account via the screening constants α and β whose values are 0.725 and 1.088, respectively.

CALPHAD

Thermodynamic assessment of U-Nb was carried out using the PARROT module of ThermoCalc. The random solution model was considered for U-Nb's constitute phases including: γ (*bcc*), α (*orthorhombic*), β (*tetragonal*) and *liquid*. The Gibbs free energies of pure elements were taken from the Scientific Group Thermodata Europe (SGTE). Considered equilibrium data include ones evaluated by Koike *et al.* [6], and from the current first-principles calculations.

The atomic mobilities and diffusivities of γ were assessed using the DICTRA software coupled to ThermoCalc. Optimization process was carried out taking into account the end-members's mobility parameters from Liu *et al.* [7], and experimental diffusivities reported in that work.

Phase-Field Modeling

To account for non-equilibrium transformation attributed to the DP, a phase-field model with finite dissipation at the interface [5] was implemented. The simulation was carried out at 450^0C, taking into account current assessed thermodynamic and kinetic data as reference. Here, the calculated interdiffusivities and atomic mobilities of γ had to be scaled up to match those derived from the experimental triple products ($sD\delta$) in [1] (assuming the segregation factor (s) is of the order of 10^{-1}, and interface width (δ) is of the order of $10^{-9} - 10^{-10}$ m). It was found that by matching the calculated interdiffusivities with experimental equivalents, simulated time and length scales can be reasonably reproduced. Interfacial mobilities were estimated according to the empirical formula: $\mu = 10^7 \frac{D_i M_i}{D_i + M_i}$, where $i = \alpha$ or γ; M is atomic mobility and D is interdiffusivity. The interfacial energies were taken to be smaller along the normal than the growth direction of the lamellae. The grid spacing was chosen to be 1.8 nm. The interfacial width was considered to be three times the grid spacing. The simulation domain is 72×72 grids. Initial compositions of γ, γ' (in 2-D simulations only), and α are 13, 47, and 3 at.% Nb, respectively. Fast grain-boundary diffusion was implemented in order to reflect the real physical condition [2].

Results and Discussions

Fundamental thermodynamics and kinetics

To verify our first-principles approaches, calculations of lattice parameters were carried out at different compositions and compared with experiments. Fig. 2 shows good agree-

ment between calculations and experiments (error $< 1\%$). The calculated formation energies of γ are shown in Fig. 3. It can be seen from this figure that the calculation results from two different density-functional approaches are in good agreement with each other. In addition, they both indicate γ's solid-solution behavior in the Nb-rich region, in phenomenological consistency with the experimental phase diagram [6]. This tends to verify the reliability of the present first-principles calculations.

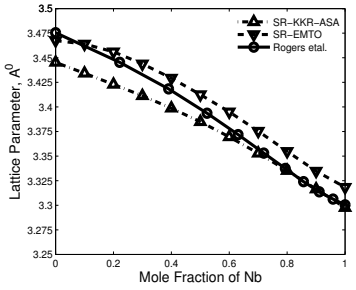

Figure 2: Calculated lattice parameter

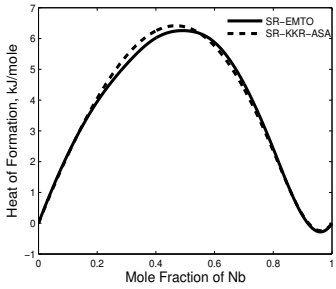

Figure 3: Calculated heats of formation

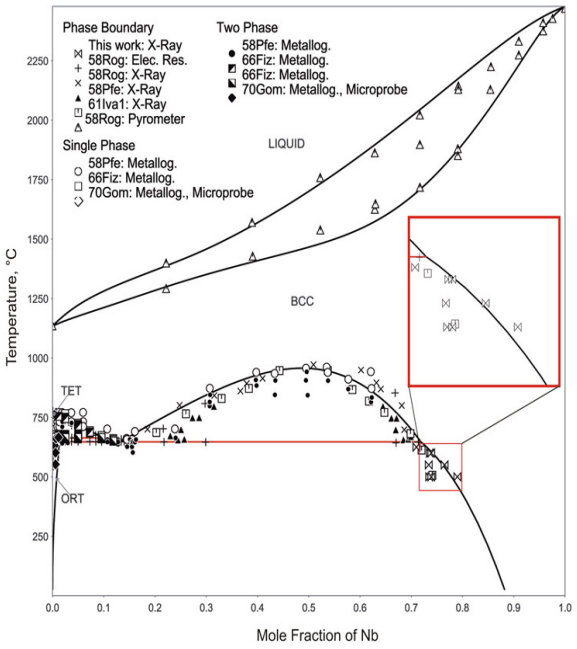

Figure 4: Calculated phase diagram

Among the two sets of formation energies, EMTO data was taken as an imposed constraints to improve the consistency of the CALPHAD thermodynamic assessment. This was done in addition to the consideration of equilibrium data taken from [6]. The calculated phase diagram, as the result of the coupling between CALPHAD and first-principles calculations, is shown in Fig. 4. As indicated in this figure, the present calculated phase diagram is reasonably consistent with previous experiments. Especially, it predicts a relatively wide 2-phase ($\alpha + \gamma$) region, deviating from all previous works. This results from the imposed *ab initio* constraints, which suggests a narrow solid-solution region, as shown in Fig. 3. Interestingly, this predicted wide ($\alpha + \gamma$) region is later verified by our x-ray experiments (see Fig. 4) on samples annealed for a longer time than done in previous works (uppermost ~ 5 years). This result much validates the use of first-principles calculations in CALPHAD assessments. To demonstrate the consistency of the present thermodynamic assessment, Gibbs formation energies of γ was back extrapolated to $0K$ and compared with the *ab initio* data. Fig. 5 (a) shows that the two sets of Gibbs formation energies are indeed reasonably compatible.

The consistent thermodynamic description was then utilized to assess the atomic mobility and diffusivity of γ. Fig. 5 (b) compares the resulting calculated interdiffusivities at 1000^0C with experiments [8] and previous calculation [7]. It can be seen from the figure that the present result agrees well with those of previous works [7, 8]. Unfortunately, due

to the limitation of available experimental data, only atomic mobilities and diffusivities of γ were evaluated in the present work. These data, however, can serve as a reference for estimating the kinetic coefficients of other phases, particularly the α phase involved in DP. Here, relying on atomic packing factor, it was assumed that atomic mobility and diffusivity of α are 3 times higher than those for γ.

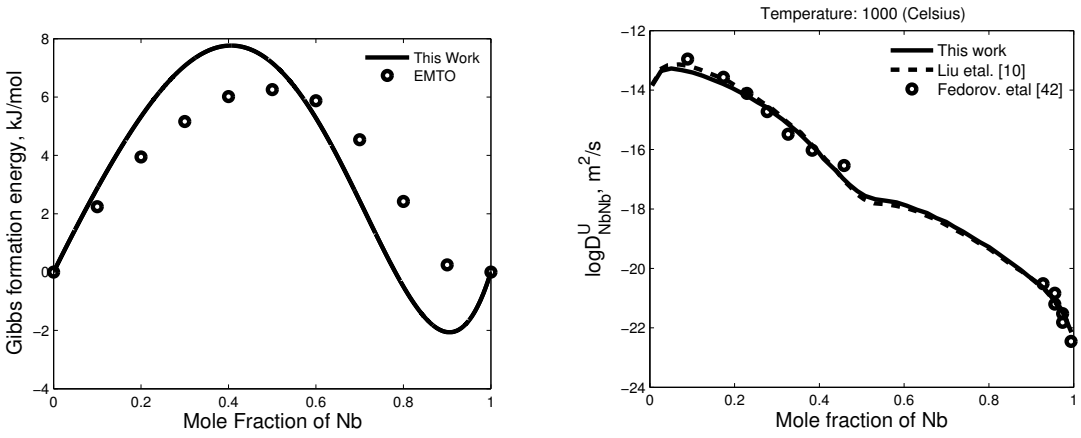

(a) (b)

Figure 5: (a) Gibbs formation energies of γ: CALPHAD vs first-principles calculations. (b) Calculated γ's interdiffusivity at 1000^0C.

Metastable γ'

It was first noted that γ' and γ share the same bcc lattice. They therefore share the same CALPHAD energetic function. Their kinetic coefficients were also chosen to be the same under the same conditions.

An initial phenomenological investigation was carried out using a 1-D diffusion couple. It is shown in Fig. 6 (dash line) that the phase-field simulation occurs according to equilibrium thermodynamics, i.e. the initial γ decomposed all the way to final products of stable α and γ_2 (stable bcc-based Nb-enrich U-Nb alloy, see Fig. 1). Investigation of the reaction's driving force however suggested that the reaction tried to converge (before the dash-line spike in Fig. 6 (b)) to some intermediate state but failed to do so. This is attributed to the absence of a local equilibrium (common tangent) between α and γ within this transitional region, as confirmed from equilibrium analysis in Fig. 7 (a).

What if there was such a local equilibrium (LE) that sustained the metastable γ', according to simple free-energy construction? This interesting question led us to the same conclusion as of Djuric [9]. Enabling such a LE during the transformation path is numerically possible. However, this requires the modification of the CALPHAD energetic profile and justification for such modification concerns us. We started considering:

- Djuric's measurements at various temperatures act as strong evidences for his argument based on simple free energy and common tangent constructions.
- Volume/lattice mismatches between α and γ introduce additional strain energy. Such addition are not explicitly taken into account in the CALPHAD assessment.

- The present assessment considered only equilibria. It should be fair if estimated equilibrium energies are reasonable; But, there is no guarantee that its energetic extrapolation into the non-equilibrium zone where DP occurs is also accurate.

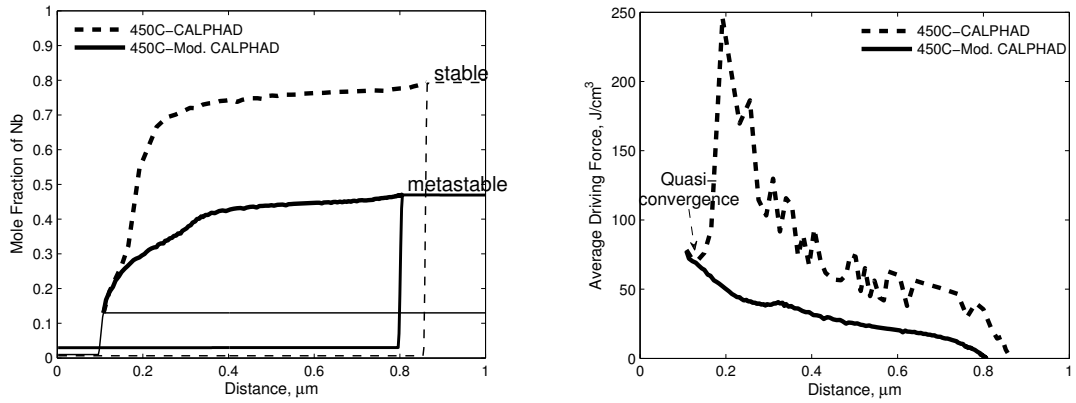

(a) (b)

Figure 6: (a) Results of 1-D diffusion-couple simulations ($\alpha|\gamma$ interface) and (b) corresponding driving forces

Based on those considerations, we proposed a new free energy profile which satisfies all reliable CALPHAD's equilibrium energetic values while accounting for additional strain energies within the CALPHAD's non-equilibrium part to achieve LE at the intermediate concentration measured by Djuric. The proposed free energy at 450^0C is shown in Fig. 7 (b). As indicated in this figure, α now forms with γ a LE at $\sim$ 47 at.% Nb, which is in good agreement with Djuric's experiment, 45 at.% Nb [9]. To describe this new free energy, piecewise cubic splines were utilized. Phase-field simulation using the proposed free energy indeed 'stabilized' the metastable phase γ' as evidenced in Fig. 6 (solid line). This suggests that strain fields around the lamellae, which tend to promote an additional LE along the decomposing path, could sustain the metastable γ' during DP.

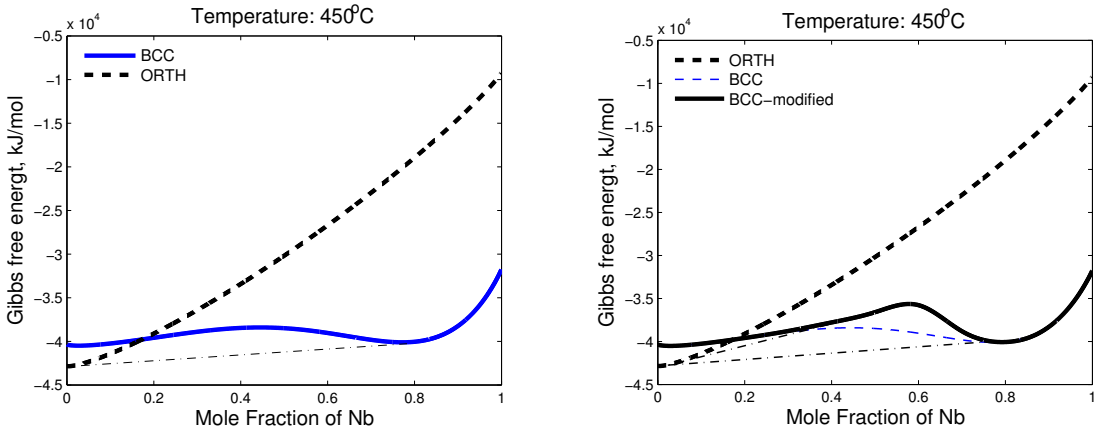

(a) (b)

Figure 7: (a) CALPHAD free energies at 450^0C. (b) Modified CALPHAD free energies at 450^0C.

2-D phase-field simulations were conducted to investigate DP's growth mechanism at 450^0C. Simulation results were reported in Fig. 8. It was interestingly found that:

- The lamellae are not likely to grow in a stable mode without considering fast grain-boundary diffusion [2], Fig. 8 (a). Under the large kinetic heterogeneity, simulated interfacial velocity and interlamellar spacing are 3.8×10^{-11} m/s and 64.8 nm compared to 5.2×10^{-11} m/s and 66 nm in [1], Fig. 8 (b).
- It can be seen from Fig. 8 (c) that significant driving forces mostly locate at the $\alpha|\gamma$ reaction fronts, indicating the role of α tips. In contrast, $\alpha|\gamma'$ interfaces are under LE condition, and do not react intensely and prevent lamellae from coalescence.
- At the $\gamma'|\gamma$ interfaces, it was expected to see completed down-hill diffusions (from γ' to γ) with equivalent composition across the interfaces and without thermodynamic driving force. However, different compositions and driving force still exist, although relatively small, and contribute slightly to the growth of γ'. This indicates that the driving force is divided into one fraction for diffusion and one fraction for moving the interfaces, which is interestingly related to Hillert's theory on DP growth [10].

From the above observations, we came up with the following explanation for the growth mechanism of DP: In U-Nb's DP, the α precipitate plays an important role. When it grows into γ, due to its lower interfacial energy with γ' than with γ, it tends to force the phase fraction of γ at the triple junction to transform into a fraction of itself and of γ' according to the equilibrium partition, i.e., α carries γ' during its growth. This carrying role of α however would not be possible if there was no fast boundary diffusion to transport, in a fast manner, the produced solute atoms around $\alpha|\gamma$ reaction fronts into γ' to guarantee the equilibrium partition. This diffusion condition also creates a 'virtual wall' of a fast anisotropic flux hindering down-hill diffusion between γ' and γ, hence maintaining the stable interface and subsequent lamellar growth. It is possible that γ' could contribute into its own growth according to [10].

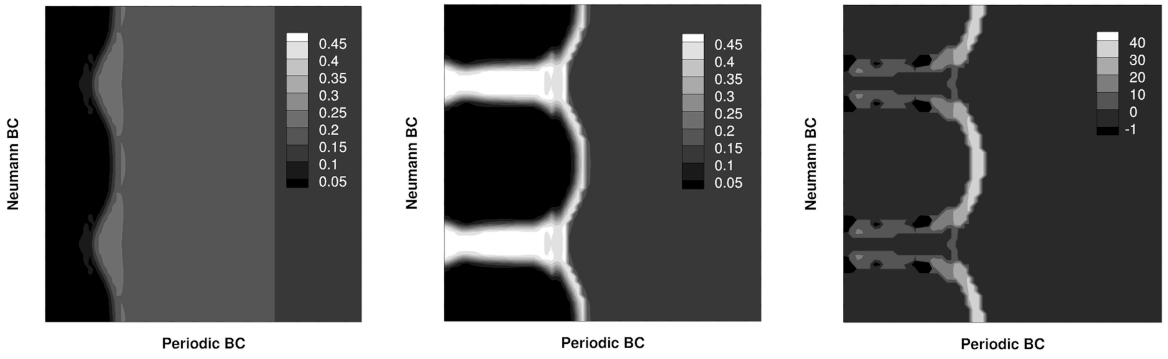

(a) (b) (c)

Figure 8: 2-D simulations of DP at 450^0C (γ (gray) $\rightarrow$ γ' (white) + α (black)). Units are mole fraction of Nb and J/cm^3 in (a, b) and (c), respectively. (a) Coalescence of α precipitates (black); (b) Stable lamellar growth; (c) Driving forces corresponding to (b).

Conclusion

In this work, we have demonstrated the implementation of a hierarchical multiscale approach to investigate the nature of the metastable monotectoid decomposition in the U-Nb system. Specifically, we used DFT calculations to extract the free energies of the solid solutions. This was then used to derive a thermodynamically consistent CALPHAD model of the entire system and subsequently mobility database for the γ phase. Finally, thermodynamic and kinetic information were integrated within the phase-field formalism to simulate the microstructure evolution during DP in U-Nb alloys. We hypothesized that (1) strain field can stabilize γ' within the lamellar structure and (2) the DP's growth mechanism is governed mainly by $\alpha|\gamma$ reaction front and the large kinetic heterogeneity.

Acknowledgements

This work was performed under the auspices of the US DOE by the LLNL and LANL under contract Nos. DE-AC52-07NA27344 and DE-AC52-06NA25396, respectively. Calculations were done using the Chemical Engineering Cluster at TAMU. REH acknowledges T.J. Tucker and P.A. Papin, and TCD acknowledges I. Steinbach and O. Shchyglo for their assistance.

References

[1] R. E. Hackenberg, H. M. Volz, P. A. Papin, A. M. Kelly, R. T. Forsyth, T. J. Tucker, K. D. Clarke, Kinetics of lamellar decomposition reactions in U-Nb alloys, Solid State Phenomena 172 (2011) 555–560.

[2] I. Manna, S. Pabi, W. Gust, Discontinuous reactions in solids, International Materials Reviews (46) (2001) 53–91.

[3] W. Kohn, Nobel lecture: Electronic structure of matter-wave functions and density functionals, Reviews of Modern Physics 71 (5) (1999) 1253–1266.

[4] L. Kaufman, H. Bernstein, Computer calculation of phase diagrams with special reference to refractory metals, Refractory Materials 4 (Academic Press, New York and London, 1970).

[5] I. Steinbach, L. Zhang, M. Plapp, Phase-field model with finite interface dissipation, Acta Materialia 60 (6) (2012) 2689–2701.

[6] J. Koike, M. Kassner, R. Tate, R. Rosen, The Nb-U (niobium-uranium) system, Journal of Phase Equilibria 19 (3) (1998) 253–260.

[7] Y. Liu, D. Yu, Y. Du, G. Sheng, Z. Long, J. Wang, L. Zhang, Atomic mobilities, diffusivities and their kinetic implications for U-X (X = Nb, Mo) bcc alloys, Calphad 37 (2012) 49–56.

[8] G.B. Fedorov, E.A. Smirnov, Diffusion in reactor materials, Tech. rep., National Bureau of Standards, Washington, DC (USA) (1984).

[9] B. Djurić, Decomposition of gamma phase in a uranium-9.5 wt.% niobium alloy, Journal of Nuclear Materials 44 (2) (1972) 207–214.

[10] M. Hillert, On theories of growth during discontinuous precipitation, Metallurgical Transactions 3 (11) (1972) 2729–2741.